Time-Warping Analysis of the T-Wave Peak-to-End Interval to Quantify Ventricular Repolarization Dispersion During Ischemia

Neurys Gómez, Julia Ramírez, Juan Pablo Martínez and Pablo Laguna *†‡§

Abstract

Background: The presence of myocardial ischemia can increase ventricular arrhythmic risk due to a raised dispersion of ventricular repolarization. This is reflected on the morphology of the T-wave on the electrocardiogram (ECG), and can be quantified by time-warping based indexes, like d_w. However, T-wave morphology can also be affected by ischemia-induced ST segment changes, impacting the accuracy of d_w. We hypothesize that ischemia-induced repolarization dispersion can be better quantified by restricting d_w to the T-wave peak-to-end (T_{pe}) interval. *Methods:* 101 ECG recordings from patients undergoing a percutaneous coronary intervention (PCI) were analyzed together with their control ECG recordings, acquired before the intervention. A series of d_w values was calculated by quantifying the T_{pe} morphological variations between the T-waves from the PCI and a reference derived from the control ECG recordings. We proposed a normalized version of d_w, $\mathcal{R}_d$, reflecting relative variations of d_w during PCI to control recordings, and compare it with traditional indices behaviour. *Results:* Values of d_w followed a gradually increasing trend as PCI inflation time progressed, reaching a median[range] $\mathcal{R}_d$ value of 9.44 [1.01, 80.74] at the occlusion end. During control recordings, d_w remained stable, with a low intra-patient standard deviation, range [0.02, 2.09] ms and a median[range] $\mathcal{R}_d$ of 1.00 [0.03, 2.93]. $\mathcal{R}_d$ at oclussion end was significantly higher than threshold values of 1, 2, 5, and 10 in 94.1%, 85.11%, 64.4% and 48.5% of patients, respectively. The spatial lead-wise analysis of d_w showed distinct distributions depending on the occluded artery, suggesting a relation with the

*This paper was submitted for review on January 17, 2024. *Asterisk indicates corresponding author.*

†N. Gómez* is with BSICoS group, I3A, IIS Aragón, University of Zaragoza, Zaragoza, Spain, and University of Oriente, Cuba (correspondence e-mail: 794826@unizar.es).

‡J. Ramírez is with BSICoS group, I3A, IIS Aragón, University of Zaragoza, Zaragoza, Spain, and with William Harvey Research Institute, Queen Mary University of London, United Kingdom.

§J. P. Martínez, and P. Laguna are with BSICoS group, I3A, IIS Aragón, University of Zaragoza, Zaragoza, and with CIBER-BBN, Spain.

ischemia location. The relative variation $\mathcal{R}$ with ischemia of index d_w (9.4) is greater than for traditional T wave amplitude (7.7), T peak-to-end interval (2.7) and T width (3.0). *Conclusions and Significance:* The index d_w, quantifying T_{pe} morphology variations, allows to follow the ischemia induced variations in repolarization in a more robust manner than classical indexes, avoiding ST segment and early T wave distortions not related to repolarization dispersion, and warranting further clinical studies to evaluate its ventricular arrhythmia risk predictive value during ischemia.

Electrocardiogram, T-wave time warping analysis, T-wave morphology, T-peak to T-end interval, ischemia, repolarization, ventricular arrhythmic risk.

1 Introduction

Heart diseases remain the leading cause of death worldwide according to the American Heart Association and European Society of Cardiology [1, 2]. In addition, experts predict that the burden of cardiovascular disease will grow exponentially over the next few years as the long-term effects of the COVID-19 pandemic evolve [3]. Cardiac arrhythmias are responsible for a great portion of the cardiac deaths. Ischemia in the cardiac tissue is a substrate which increases the risk for ventricular arrhythmias, including ventricular tachycardia and ventricular fibrillation [4].

One of the mechanisms that increase propensity to arrhythmia under ischemia is the increased dispersion of ventricular repolarization. The link between heterogeneities resulting in dispersion of ventricular repolarization and the genesis of arrhythmias has been demonstrated both in experimental models and in clinical studies [5, 6]. However, robustly identifying in the ECG those markers of repolarization alterations that better represents the potentially harmful substrate remains an unmet demand. This challenge can also be dependent on the pathologies generating the risk.

This work will concentrate on the study of arrhythmia risk from the ECG under ischemic conditions. It must be noted that many arrhythmia risk ECG biomarkers developed for non-ischemic conditions (e.g. long QT syndrome, brugada syndrome, chronic heart failure, etc.) are challenged under ischemic conditions by the presence of concurrent ST elevation/depression and early T-wave modifications which appear at the ECG simultaneously with the arrhythmia risk signatures.

ECG changes during acute ischemia include alterations in the ST-segment level and/or T-wave amplitude [7], together with alterations of the global spatio-temporal characteristics of the ECG. Those alterations have been the basis for the development of ischemia detectors and monitoring systems, being the ST-level the most widely-used [8]. However, while in some patients mild to moderate ischemia can cause low alteration on the ECG, more pronounced ST elevation/depression can occur during severe ischemia largely affecting the early part of the T-wave on the ECG [7, 9, 10]. So, it is important to consider these

manifestations of ischemia in the selective development of biomarkers quantifying the degree of repolarization dispersion as a surrogate for arrhythmia risk under ischemia.

Acute ischemia induced during Percutaneous Coronary Intervention (PCI) provides an excellent model to investigate the dispersion of repolarization changes undergoing during the initial minutes of ischemia. It alters ventricular repolarization by, (a) shortening repolarization time (i.e., temporal changes) and (b) slowing the conduction speed [9], creating heterogeneity between different myocardial regions. Ischemia-induced heterogeneity has been related to the generation of ventricular arrhythmias and increased arrhythmic risk [11, 12]. However, other ischemia-induced changes in the ECG unrelated to repolarization dispersion, such as ST elevation/depression may interfere in the computation and interpretation of risk markers developed for non-ischemic scenarios, such as T-wave alternans [13], the V-index [14] or the T-wave morphology restitution (TMR) [15] or variation (TMV) [16].

Several biomarkers have been proposed to quantify the spatio-temporal heterogeneity of repolarization, such as the QT interval [17], T-wave width [6], the distance from the peak to the end of the T-wave (T_{pe} interval) [18, 19], dynamic changes in the T_{pe} interval with respect to heart rhythm [20], QT interval variability [12], T-wave alternans [21], QT memory lag [22], or ST elevation [23]. Most of these markers are based on measurements relying solely on the determination of ECG fiducial points, therefore not capturing all the information conveyed on the morphology of the T-wave. Other biomarkers have been proposed trying to overcome this limitation: The information provided by the vectorcardiogram is used in [24] and the V-index is proposed in [14]. Moreover, the T-wave morphology restitution index (TMR) quantifies the morphological variations of the T-wave with respect to heart rate changes [15] using the warping-based index d_w. TMR was later modified to quantify T-wave morphology variation with respect to a population-defined reference (TMV index) [16].

Under ischemic conditions, the ST elevation/depression may largely influence the above-described markers, reducing their accuracy in quantifying arrhythmic risk, limiting their utility. This is not the case for the T-peak to T-end interval, although this marker is still largely sensitive to errors in the identification of the fiducial points. To overcome these restrictions, we hypothesize that a global T-wave morphology analysis as the one presented in [15], but restricted to the T-peak to T-end part of the T-wave, can be a proper, robust and artefact-free alternative to quantify repolarization dispersion during ischemia as surrogate of the ischemia induced arrhythmic risk.

The main novelty in this study, with respect to the state-of-the-art, is the particularization of the time-warping-based methodology for the quantification of repolarization dispersion to the final part of the T wave, thus avoiding the ST segment shift influence on the computation of d_w in ischemic conditions. Other methodological novelties are the use of a running Mean Warped T_{pe} (MWTPE) estimation along the recordings, together with a reference MWTPE election criteria, and the comparison of the repolarization dispersion quantification ability of the new version of the d_w marker with that of other classic ischemia indices.

2 Materials and Methods

2.1 Data set

The study population contained 101 patients from the STAFF III database [25] (63 males, with 35 patients with evidence of prior myocardial infarction) undergoing elective balloon percutaneous coronary intervention (PCI). The database was collected at the Charleston Area Medical Center (WV, USA), where single prolonged balloon inflation had been introduced to achieve optimal results of the PCI. Standard leads V1–V6, I, II, and III of the ECG were digitized with an amplitude resolution of 0.625 μV and a sampling rate of 1000 Hz. The remaining three standard augmented leads aVL, -aVR, and aVF were subsequently generated from the limb leads and used for the spatial analysis. The study was approved by the local Investigational Review Board and informed consent was obtained from the patients before their enrolment. All patients were clinically stable during the ECG acquisition. Patients who presented any signal loss during the recording were not included.

For each patient, 5 minutes ECG recording at rest in supine position previous to any catheter insertion or balloon inflation (control recording) and the corresponding paired ECG recording obtained during the first balloon inflation were analyzed. The duration of the occlusion period ranged from 1:09 to 7:17 minutes (mean: 4:20 minutes). The spatial distributions of the 101 balloon inflations were: left main (LM) artery in 2 patients, left anterior descending (LAD) artery in 33 patients, left circunflex artery (LCX) in 21 patients and right coronary artery (RCA) in 45 patients, distribution with each artery can be found in Table 2.

2.2 ECG Pre-processing

The following steps were performed in the ECG pre-processing. First, the ECG signal was filtered with a low-pass sixth-order bidirectional Butterworth filter at 40-Hz cut-off frequency to attenuate electric and muscle noise, and with a sixth-order high-pass bidirectional Butterworth filter at 0.5-Hz cut-off frequency to attenuate baseline wander. Second, a wavelet-based single-lead QRS delineator [26] was used to determine the QRS fiducial points for each of the nine leads (V1-V6, I, II and III). Then, unique multilead QRS fiducial points were obtained from the 12 single-lead sets of onsets and ends, using a multi-lead selection rule strategy [27]. Third, spatial Principal Component Analysis (PCA) transformation was performed on the eight independent leads to emphasize T-wave components and improve its delineation. The PCA transformation coefficients were restrictively calculated from the T-wave segment, and were obtained as the eigenvectors of the 8x8 interlead auto-correlation matrix computed over the T-waves contained in a 15-second window at the beginning of the recording, for control recordings, or at beginning of the balloon inflation, for PCI recordings. T-wave segmentation was done at fixed distances referred to the corresponding QRS mark following rules in [28]. Fourth, the first principal component

ECG signal, i.e., the transformed lead where the T-waves have maximal energy, was delineated making use of the single-lead technique [26]. The resulting fiducial points were used for the subsequent ECG analysis. Finally, each T-wave was further filtered with a sixth order low-pass bidirectional Butterworth filter (cut-off frequency of 20 Hz) in order to remove the remaining out-of-band high frequency components.

2.3 Quantification of T-wave morphology changes

Each recording was divided into consecutive 15-second windows, with 10 seconds overlap. For each s-th window, a mean warped T-wave (MWTW) [15] restricted to the T-peak to T-end interval (MWTPE) was computed, $\boldsymbol{f}^s(\boldsymbol{t}^s) = [f^s(t^s(1)), ..., f^s(t^s(N_s))]^T$, where $\boldsymbol{t}^s = [t^s(1), ..., t^s(N_s))]^T$, as shown in Fig. 1a. Initially, all T-waves contained within a given window were transformed to have positive polarity. For each window, the predominant T-wave class, biphasic or monophasic, was determined as the one with the highest number of occurrences. Only T-waves from the predominant class were considered for the computation of the MWTPE.

Selected T peak to end waves are aligned with respect to the T-wave peak. Additionally, an extra selection rule was applied to avoid the effect of delineation errors: only those T-waves whose duration T_w satisfies $T^s_{w,m} - 40 \leq T_w \leq T^s_{w,m} + 40$ (ms) were selected for the MWTPE computation, where $T^s_{w,m}$ is the median of the T-wave duration within each s-th window. The estimated MWTPE $\boldsymbol{f}^s(\boldsymbol{t}^s)$ is representative of the dominant morphology of T-waves from peak to end in that particular s-th window.

We chose a reference MWTPE among the $\boldsymbol{f}^s$ MWTPEs from the first minute in the case of the control recording, and from the first 30 seconds after balloon inflation in case of the PCI recordings, $\boldsymbol{f}^r(\boldsymbol{t}^r)$ in Fig. 1b, (blue dashed line rectangle). The selection period at PCI recordings is smaller to minimize ischemia-induced repolarization changes. To choose the reference MWTPE $\boldsymbol{f}^r(\boldsymbol{t}^r)$ from the most stable s-th time window, we compute a dispersion index (υ_s) in each s-th window, as:

$$\upsilon_s = \frac{\dfrac{1}{N_s}\dfrac{1}{M_s}\displaystyle\sum_{i=1}^{M_s}\left[\boldsymbol{f}_i^s(\boldsymbol{t}^s) - \boldsymbol{f}^s(\boldsymbol{t}^s)\right]^{\mathrm{T}}\left[\boldsymbol{f}_i^s(\boldsymbol{t}^s) - \boldsymbol{f}^s(\boldsymbol{t}^s)\right]}{\dfrac{1}{N_s}\left[\boldsymbol{f}^s(\boldsymbol{t}^s)\right]^{\mathrm{T}}\boldsymbol{f}^s(\boldsymbol{t}^s)}, \tag{1}$$

considering all pieces of T-waves $\boldsymbol{f}_i^s(\boldsymbol{t}^s)$ ($i \in \{1 \dots M_s\}$) within each window. Then, the reference MWTPE is taken as

$$\boldsymbol{f}^r(\boldsymbol{t}^r) \equiv \boldsymbol{f}^{s_m}(\boldsymbol{t}^{s_m}), \quad \text{with} \quad s_m = \arg\min_s\{\upsilon_s\}. \tag{2}$$

To quantify the evolution of the MWTPEs morphology along time in each patient we applied the method originally proposed by Ramírez *et al.* [15], which estimated the index d_w as the mean amount of warping needed to remove the time domain variation among two different waves, the reference $\boldsymbol{f}^r(\boldsymbol{t}^r)$, and the

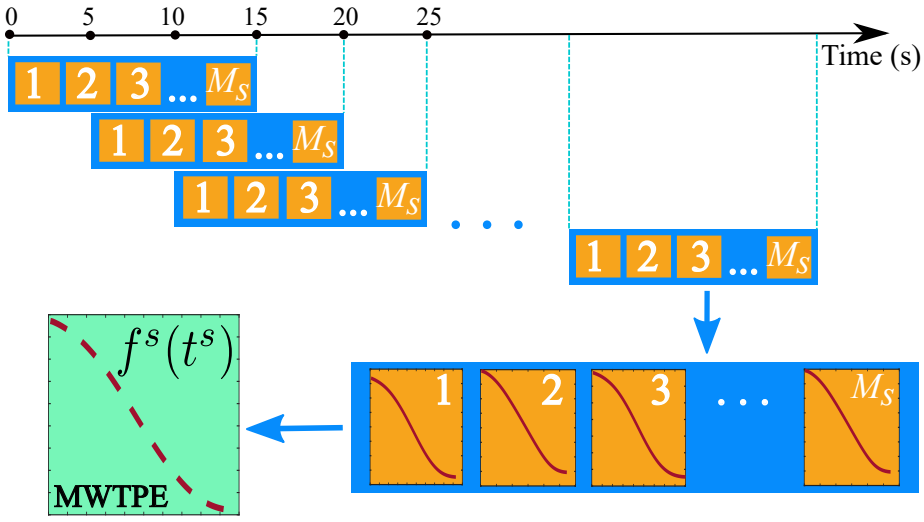

(a)

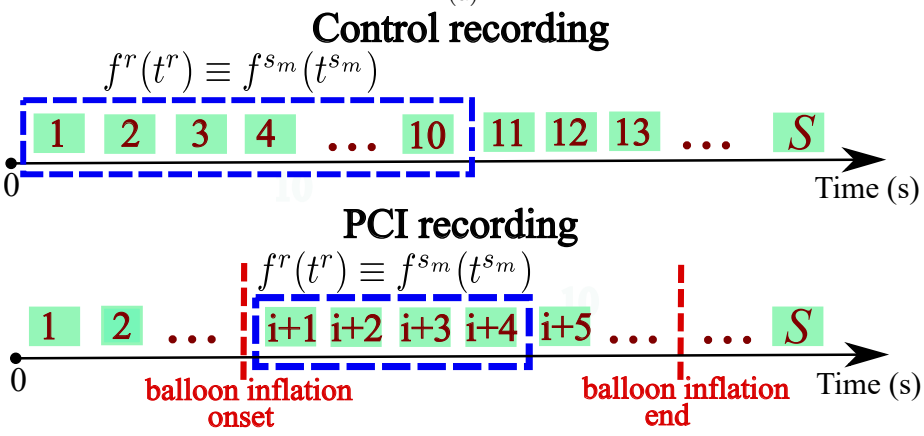

(b)

Figure 1: MWTPE $\boldsymbol{f}^s(\boldsymbol{t}^s)$ estimation and reference MWTPE $\boldsymbol{f}^r(\boldsymbol{t}^r)$ selection rule at the STAFF-III data-set. The $\boldsymbol{f}^s(\boldsymbol{t}^s)$ MWTPE was estimated from time-windows of 15 seconds duration and 10 seconds of overlap throughout the entire record. The reference $\boldsymbol{f}^r(\boldsymbol{t}^r)$ MWTPE was selected among the MWTPEs within 1 minute period, at the control recording, and within 30 seconds period at the beginning of the PCI recordings.

one under study $\boldsymbol{f}^s(\boldsymbol{t}^s)$. Fig. 2a shows an example of the MWTPEs previous to time-warping, $\boldsymbol{f}^r(\boldsymbol{t}^r)$ calculated at the initial part of a PCI recording and $\boldsymbol{f}^s(\boldsymbol{t}^s)$ from two minutes later.

Let $\gamma(\boldsymbol{t}^r)$ be the warping function that relates $\boldsymbol{t}^r$ and $\boldsymbol{t}^s$ such as the composition $[\boldsymbol{f}^s \circ \gamma](\boldsymbol{t}^r) = \boldsymbol{f}^s(\gamma(\boldsymbol{t}^r))$ denotes the time-warping or re-parameterization of the $\boldsymbol{f}^s(\boldsymbol{t}^s)$ using $\gamma(\boldsymbol{t}^r)$. As in [15], the square-root slope function (SRSF) was

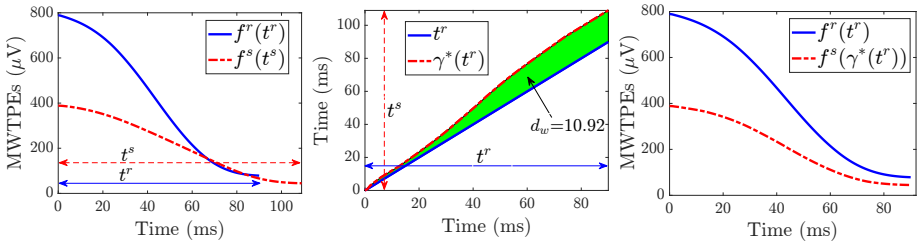

(a) (b) (c)

Figure 2: Analysis performed for time-warping index estimation from a particular patient of the STAFF-III database during the PCI procedure. Panel (a) displays both the reference $\boldsymbol{f}^r(\boldsymbol{t}^r)$ (solid blue) and a particular s-th $\boldsymbol{f}^s(\boldsymbol{t}^s)$ (doted red line) MWTPE. Panel (b) displays the warping function $\gamma^*(t^r)$ (dotted red line) that optimally relates the reference $\boldsymbol{f}^r(\boldsymbol{t}^r)$ and studied $\boldsymbol{f}^s(\boldsymbol{t}^s)$ MWTPEs. The total amount of warping, quantified by d_w, is represented by the green area between $\gamma^*(t^r)$ and t^r. Panel (c) displays both the reference $\boldsymbol{f}^r(\boldsymbol{t}^r)$ (blue line) MWTPE and the warped $\boldsymbol{f}^s(\gamma(\boldsymbol{t}^r))$ MWTPE.

used to find the optimal warping function, and hence avoiding any potential "pinching effect". The SRSF is obtained as the square-root of the derivative of $\boldsymbol{f}(\boldsymbol{t})$, considering the sign:

$$\boldsymbol{q}_f(\boldsymbol{t}) = sign\left(\dot{\boldsymbol{f}}(\boldsymbol{t})\right)\sqrt{|\dot{\boldsymbol{f}}(\boldsymbol{t})|}. \tag{3}$$

The fuction, $\gamma^*(\boldsymbol{t}^r)$, that minimizes the amplitude difference between the SRSF of $\boldsymbol{f}^r(\boldsymbol{t}^r)$ and $\boldsymbol{f}^s(\gamma(\boldsymbol{t}^r))$, $\boldsymbol{q}_{f^r}(\boldsymbol{t}^r)$ and $\boldsymbol{q}_{[\boldsymbol{f}^s\circ\gamma]}(\boldsymbol{t}^r) = \boldsymbol{q}_{f^s}(\gamma(\boldsymbol{t}^r))\sqrt{\dot{\gamma}(\boldsymbol{t}^r)}$, respectively, is selected as the optimal warping function [29, 30],

$$\begin{aligned}\gamma^*(\boldsymbol{t}^r) &= \underset{\gamma(\boldsymbol{t}^r)}{\arg\min}\left(\|\boldsymbol{q}_{f^r}(\boldsymbol{t}^r) - \boldsymbol{q}_{|f^s\circ\gamma|}(\boldsymbol{t}^r)\|\right)\\ &= \underset{\gamma(\boldsymbol{t}^r)}{\arg\min}\left(\|\boldsymbol{q}_{f^r}(\boldsymbol{t}^r) - \boldsymbol{q}_{f^s}(\gamma(\boldsymbol{t}^r))\sqrt{\dot{\gamma}(\boldsymbol{t}^r)}\|\right).\end{aligned} \tag{4}$$

To obtain this optimum the dynamic programming algorithm [31] was used to optimise the analysis, explained in detail in Appendix A in [15]. The warping function $\gamma^*(\boldsymbol{t}^r)$, that optimally relates $\boldsymbol{f}^s(\boldsymbol{t}^s)$ and $\boldsymbol{f}^r(\boldsymbol{t}^r)$ in Fig. 2a is shown in Fig. 2b. The warped T peak to end wave, $\boldsymbol{f}^s(\gamma(\boldsymbol{t}^r))$, and the reference $\boldsymbol{f}^r(\boldsymbol{t}^r)$, are shown in Fig. 2c.

The index d_w is defined to quantiy the time-warping level needed to optimally align the T peak to end waves (MWTPE) as the average of the absolute differences between $\gamma^*(\boldsymbol{t}^r)$ and $\boldsymbol{t}^r$:

$$d_w = \frac{1}{N_r}\sum_{n=1}^{N_r}|\gamma^*(\boldsymbol{t}_r(n)) - \boldsymbol{t}^r(n)|. \tag{5}$$

In order to analyze the d_w time course during acute ischemia, its value was computed for each s-th $\boldsymbol{f}^s(\boldsymbol{t}^s)$ MWTPE, resulting in the time series $d_w(s)$.

2.4 Repolarization changes analysis

The analysis of repolarization changes is performed in two different ways:

1. Temporal evolution: The warping is performed on the first principal component transformed lead since it is supposed to emphasize T-wave components and so hypothesized to enhance morphological differences. For each patient, the time course variation of repolarization dispersion is evaluated as the evolution of $d_w^{\text{PCA}}(s)$, $s \in \{1, \ldots, S\}$, every 5 seconds relative to the initial stage taken at reference.

2. Spatial distribution: We separately quantified $d_w(s)$ in each of the 12 standard leads, and investigated the relationship between the occlusion site and spatial distribution of the $d_w^{\text{L}}(s)$, L$\in$ {V1,...,V6, aVL, I, aVR, II, aVF, III}. To have a spatially global indication of warping, the mean across patients of $d_w^{\text{L}}(s)$ maximum in each PCI recordings, is also computed and denoted $\overline{d}_w^{\text{L}}(s)$.

To analyze the warping value evaluated at any time of the PCI intervention, the value $d_w(s)$ is expressed in relative terms with respect to d_w variations during the ischemia free control recording using the index $\mathcal{R}_d$. Similar to the ischemic changes sensor proposed in [8], $\mathcal{R}_d$ normalizes the change induced by ischemia using the standard deviation of d_w measured at the control recording, where no ischemic-induced changes are expected, denoted as σ_d^c.

The $\mathcal{R}_d$ in this study is defined as,

$$\mathcal{R}_d(s) = \frac{\Delta_d^{\text{PCI}}(s)}{\sigma_d^c}, \tag{6}$$

where the magnitude of change in $d_w(s)$ during PCI occlusion at any time, s, is denoted by $\Delta_d^{\text{PCI}}(s)$. In order to have a robust estimation of $\Delta_d^{\text{PCI}}(s)$, a linear fitting model $\hat{d}_w(s)$ is fit to $d_w(s)$ between $s = 1$ and s and defining $\Delta_d^{\text{PCI}}(s)$ as the difference between $\hat{d}_w(s)$ and $\hat{d}_w(1)$. For example, a value of $\mathcal{R}_d = 5$ means that the $d_w(s)$ has increased during the occlusion 5 times the standard deviation of the change observed during the control recording σ_d^c.

2.5 Classical indices of ventricular repolarization

To further test the robustness of d_w, we compare its performance with that from the following traditional ischemic indices:

- ST segment level (ST): Measured as the difference between the ECG signal amplitude at time instant 60 ms after the J point and the isoelectric level, computed as the signal averaged over a 10 ms segment starting 15 ms before the QRS onset.

- T-wave peak amplitude (T_a): Amplitude difference between the T-wave peak fiducial point and the isoelectric segment.

- T-wave width ($\mathrm{T_w}$): Interval from T-onset to T-end points.
- T-wave peak to end interval (T_{pe}): Interval from T-peak to T-end time instants of the T-wave.

Each index was measured beat-to-beat to analyze its time course during PCI, obtaining the series $\mathrm{ST}(n)$, $\mathrm{T}_a(n)$, $\mathrm{T_w}(n)$ and $\mathrm{T}_{pe}(n)$, respectively. We also analyzed the magnitude of changes observed during balloon inflation for each patient using $\mathcal{R}_{\mathcal{I}}^{\mathrm{PCA}}$, defined analogously to $\mathcal{R}_d^{\mathrm{PCA}}$ in (6), where $\mathcal{I} \in \{\mathrm{ST}, \mathrm{T}_a \mathrm{T_w}, \mathrm{T}_{pe}\}$.

2.6 Statistical analysis

McNemar analysis was used to compare control with PCI recordings, and Fisher's exact test was used in the contingency tables. We used the Kruskal-Wallis test to assess differences among groups. The statistical significance was considered when p-value ≤ 0.05. We used boxplots to show the distributions of data, where the central mark represents the median, the edges represent the 25th and 75th percentiles, and the whiskers represent the most extreme data points not considered as outliers. Computations were made with MATLAB® version R2020b.

3 Results

3.1 Changes of d_w during occlusion

When computing d_w for each s-th window and each individual patient the percentage of T waves that do not satisfy the extra selection rule related to T wave duration ($T_{w,m}^s - 40 \leq T_w \leq T_{w,m}^s + 40$ (ms)), was, in average, 1,4%.

In the control recording, the standard deviation, σ_d^c, had a median of 0.54 [IQR: 0.33], ranging from 0.018 to 2.085 ms. The stability of d_w in the control recording was tested by estimating $\mathcal{R}_d^{\mathrm{PCA}}$ in the second half of each control record using as reference the value obtained in its first half, showing a median of 1.00 [IQR: 1.13], ranging from 0.03 to 2.93.

The number of patients, for control and PCI stage, where $\mathcal{R}_d^{\mathrm{PCA}}$, evaluated as in (6) with $s = s^{\mathrm{PCIend}}$, is larger than certain thresholds (1, 2, 5 and 10) are reported in Table 1. Percentages of recordings with $\mathcal{R}_d^{\mathrm{PCA}}$ over a threshold in PCI, were found significantly higher than in control: $\mathcal{R}_d^{\mathrm{PCA}} > 1, 2, 5, 10$, in 94.1%, 85.11%, 64.4% and 48.5 % of PCI recordings vs 50.5% 12.9%, 0% and 0% in control, McNemar test $p = 3.7 \cdot 10^{-11}$, $p = 4.0 \cdot 10^{-21}$, $p = 5.4 \cdot 10^{-20}$ and $p = 3.6 \cdot 10^{-15}$, respectively. Details of $\mathcal{R}_d^{\mathrm{PCA}}$ prevalence during PCI recordings segregated by occluded artery, gender and the presence of previous MI are reported in Table 2.

We did not find any significant differences in prevalence of repolarization changes, measured as $\mathcal{R}_d^{\mathrm{PCA}} > 2$, by occlusion site: 81.8%, 86.7%, and 85.7% for LAD, RCA and LCX, respectively. LM group was excluded in this comparison due to its small size. For larger, $\mathcal{R}_d^{\mathrm{PCA}} > 5$, changes requirements, patients with LAD occlusion reached the threshold in 66.7% of the patients and RCA

Table 1: $\mathcal{R}_d^{\text{PCA}}$ prevalence classification in the study population according to the stage test

Subset	#	$\mathcal{R}_d^{\text{PCA}} > 1$	$\mathcal{R}_d^{\text{PCA}} > 2$	$\mathcal{R}_d^{\text{PCA}} > 5$	$\mathcal{R}_d^{\text{PCA}} > 10$
Control recording	101	51 (50.5%)	13 (12.9%)	0	0
PCI * recording	101	95 (94.1%)	86 (85.11%)	65 (64.4%)	49 (48.5%)

* $p \leq 0.05$ PCI recordings vs Control recordings (McNemar test)

Table 2: $\mathcal{R}_d^{\text{PCA}}$ prevalence classification in the study population according to the occluded artery, gender, and evidence of previous infarction.

Subset	#	$\mathcal{R}_d^{\text{PCA}} > 1$	$\mathcal{R}_d^{\text{PCA}} > 2$	$\mathcal{R}_d^{\text{PCA}} > 5$	$\mathcal{R}_d^{\text{PCA}} > 10$
LAD	33	31 (94.0%)	27 (81.8%)	22 (66.7%)	15 (45.5%)
diag	2	1	1	1	0
mid	6	6	4	3	2
prox	22	21	19	16	13
prox-mid	3	3	3	2	0
RCA	45	42 (93.3%)	39 (86.7%)	32(71.1%)	25 (55.6%)
dist	12	12	11	9	9
mid	14	12	12	8	4
prox	17	16	15	14	12
prox-mid	2	2	1	1	0
LCX	21	20 (95.2%)	18 (85.7%)	11 (52.4%)	9 (42.9%)
dist	6	6	6	4	2
mid	5	5	5	2	2
prox	10	9	7	5	5
LM	2	2 (100%)	2 (100%)	0	0
Male	63	60 (95.2%)	55 (87.3%)	42 (66.7%)	35 (55.6%)
Female	38	35 (92.1%)	31 (81.6%)	23 (60.5%)	14 (36.8%)
Pre-MI	35	32 (91.4%)	29 (82.9%)	20 (57.1%)	17 (48.6%)
No pre-MI	66	63 (95.5%)	57 (86.4%)	45 (68.2%)	32 (48.5%)

in 71.1% while LCX reaches the threshold just at 52.4%, of patients even the differences are not significant. Neither were significant differences in prevalence for $\mathcal{R}_d^{\mathrm{PCA}} > 10$.

Differences in the three subsets between the prevalence in men and women (63 and 38 patients in total, respectively) and between patients with and without evidence of a previous myocardial infarction (MI) (35 and 66, respectively) were not either statistically significant.

The $\mathcal{R}_d^{\mathrm{PCA}}$ magnitude ranged from 1.01 to 80.74 (mean/median: 17.55/9.44). The box and whiskers plots according to the occluded artery subsets are shown in Fig. 3. There were no significant differences between the groups ($p = 0.47$ Kruskal-Wallis test), although the largest interquartile range was found for the LAD subset.

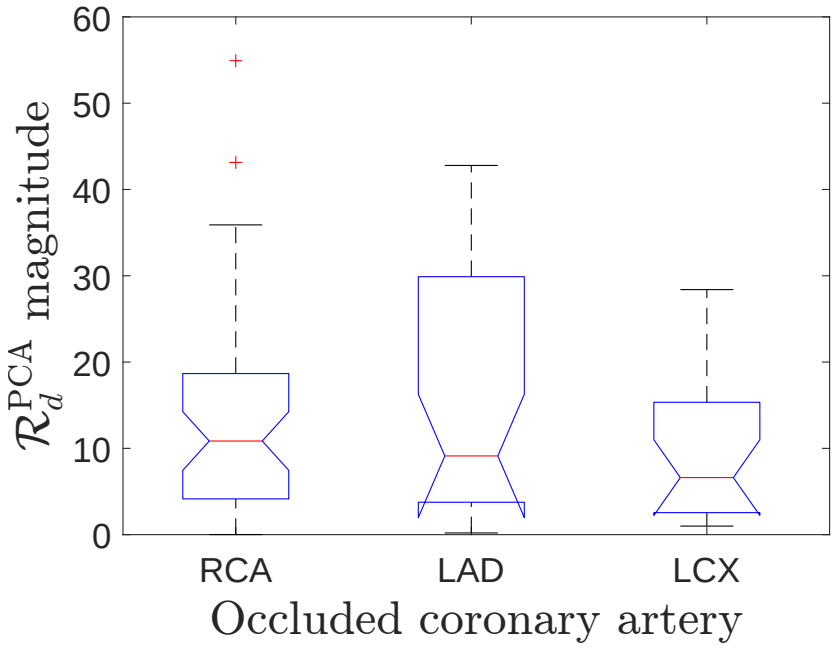

Figure 3: Box and whisker plots of the $\mathcal{R}_d^{\mathrm{PCA}}$ amplitudes in each patient classified by occluded artery.

3.2 Temporal Distribution Analysis

An example of the $d_w^{\mathrm{PCA}}(s)$ temporal evolution for a particular patient during control and PCI periods is shown in Fig. 4a. The red trace represents, for an illustrative patient, the balloon inflation time-span. Different time instants (tagged with letters) are selected to display in Fig. 4c the original T-wave shape. Strong T-wave peak-to-end shape variations accompanied by $d_w^{\mathrm{PCA}}(s)$ magnitude changes (ranging from 0 to 10.10 ms) were observed, which follow an increasing trend as inflation time progresses. In contrast, $d_w^{\mathrm{PCA}}(s)$ magnitude during

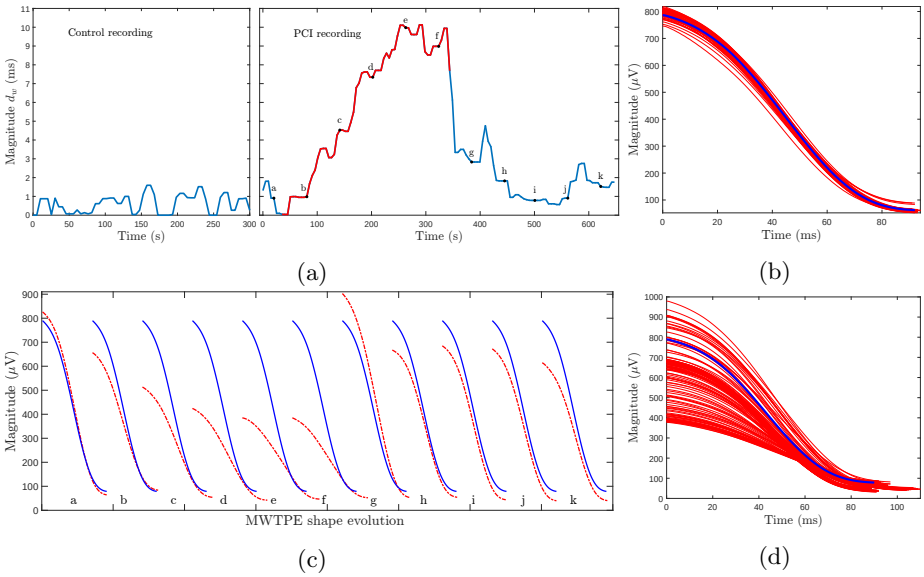

Figure 4: Example of time course evolution of $d_w^{\mathrm{PCA}}(s)$ series and T-wave peak-to-end shape changes during control and PCI stages from a particular patient. Panel (a) displays $d_w^{\mathrm{PCA}}(s)$ evolution, where the balloon inflation time is highlighted with a red line. The shape of both the reference $\boldsymbol{f}^r(\boldsymbol{t}^r)$ MWTPE (solid blue) and each s-th $\boldsymbol{f}^s(\boldsymbol{t}^s)$ MWTPE (red dashed line) are shown in panel (c), with letters indicating their corresponding time instants tagged in (a). Panels (b) and (d) show the $\boldsymbol{f}^s(\boldsymbol{t}^s)$ MWTPEs (red lines) corresponding to the $d_w^{\mathrm{PCA}}(s)$ series for the control and PCI stages, respectively. The blue line represents the reference $\boldsymbol{f}^r(\boldsymbol{t}^r)$ MWTPE. Note that the $d_w^{\mathrm{PCA}}(s)$ value at the end of the occlusion has already started to decrease. This is a consequence of the 15-second window, centered at the analysing point, which enters in the computation of $\boldsymbol{f}^s(\boldsymbol{t}^s)$ and then already introducing parts where the ischemia is reducing

control remains stationary, ranging from 0 to 1.8 ms. All $\boldsymbol{f}^s(\boldsymbol{t}^s)$ MWTPEs corresponding to the $d_w^{\mathrm{PCA}}(s)$ series in the control and PCI stages are shown in Fig. 4b and Fig. 4d, respectively. Dotted red line represents the reference $\boldsymbol{f}^r(\boldsymbol{t}^r)$ MWTPE. Note that the $d_w^{\mathrm{PCA}}(s)$ evolution described above follows the changes in the $\boldsymbol{f}^s(\boldsymbol{t}^s)$ MWTPEs shape. No significant changes are found in the control recording, while an increase in width and a decrease in amplitude of the $\boldsymbol{f}^s(\boldsymbol{t}^s)$ MWTPEs are observed in the balloon inflation period, as reflected in the $d_w^{\mathrm{PCA}}(s)$ trace in Fig. 4a.

The $d_w^{\mathrm{PCA}}(s)$ averages across all patients (blue line), denoted as $\overline{d}_w^{\mathrm{PCA}}(s)$ and segregated by occluded coronary artery, aligned to the recording onset or to the balloon inflation onset, for control and PCI recordings, respectively, are shown in Fig. 5. All database recordings were averaged. Note that the averages have little significance from the 5-th minute onwards, due to the quick decline in

number of available records, Fig. 5b.

In the 86 recordings showing $\mathcal{R}_d^{\text{PCA}} > 2$, the timing when this level of change is first reached (evaluating $\mathcal{R}_d^{\text{PCA}}$ as in (6) but with Δ_d^{PCI} computed from the linear fit of $d_w^{\text{PCA}}(s)$ just up to a given s) had a median of 15 s [IQR: 15], ranging from 5 s to 4 min 50 s. Of these, 69 patients reached $\mathcal{R}_d^{\text{PCA}} > 2$ during the first 30 seconds (80.23%), while only 9 (10.47%) and 8 (9.30%) reached it between 30 and 60 seconds, and after 60 seconds, respectively. Analysing the time course evolution of the $d_w^{\text{PCA}}(s)$ maximum in these 86 recordings we observe that 31.40% of the maximum $d_w^{\text{PCA}}(s)$ amplitude was already reached in the first two minutes after balloon inflation, and extra 32.56% was reached in the following two minutes, while the remaining 36.05% was obtained after the 4-th minute of occlusion.

3.3 Spatial Distribution Analysis

The $d_w^l(s)$ and corresponding $\mathcal{R}_d^l$ magnitude was studied in each l-th lead. The percentage of patients presenting $\mathcal{R}_d^l > 2, 5, 10$ in each lead, segregated by occluded artery, is shown in Fig. 6 by blue, red and orange bars, respectively.

$\mathcal{R}_d^l > 2$ reached a prevalence of 60% in all leads of each subset, except for l being V4 and V5 in LCX and LDA occluded artery subsets, respectively. In the RCA subgroup, elevated $\mathcal{R}_d^l$ index reached a higher prevalence in leads $l \in \{\text{V1-V3}, \text{I}, \text{aVR}, \text{aVF}, \text{III}\}$ for $\mathcal{R}_d^l > 5$ and $\mathcal{R}_d^l > 10$. A similar outcome can be seen for LAD occlusion in the same chest leads and V6 where the prevalence increases, unlike the RCA group aVR and III (inferior wall) decreases. Note that aVR reached the highest values only in the RCA group, which gives an idea of the location of the damaged ischemic region. Interestingly, for V4 (anterior wall, which corresponding to LAD area) in $\mathcal{R}_d^l > 5$ range, low values were obtained in all occluded artery groups, although it is worth noting that for LAD subgroup reached the higher prevalence.

The average lead distributions of the maximum d_w^l for RCA, LAD and LCX occlusions, $\overline{d}_w^l$, are shown in Fig. 7. According to the wall that the leads looks at and the occluded artery, the highest $\overline{d}_w^l$ values at chest leads are obtained in V1-V3 in the LAD and RCA groups (V1 in RCA with the highest values) and in V4-V6 for LCX group. Regarding limb leads, the highest values in the RCA group are obtained in I, III, and aVR. In LAD group the highest values are obtained in the augmented leads and the lowest in the limb leads. In LCX which irrigates the anterior-superior and lateral sides, high values are obtained similar to their upper chest leads V5-V6 in all limb leads (aVR, II and aVF with the highest values).

3.4 Classic Local Measurements

The time series of the different T_a, T_{pe}, T_w and ST indices were estimated, and the corresponding $\mathcal{R}_\mathcal{I}^{\text{PCA}}$ parameters were obtained at the end of occlusion to describe how ischemic variations are reflected in each index. As for the d_w

index, the $\mathcal{R}_{\mathcal{I}}^{\text{PCA}}$ estimator was evaluated using the control recording to quantify changes of each index in the control stage. The standard deviation in the first half of the control recording, $\sigma_{\mathcal{I}}^{c}$, had a median of 1.29, 0.65, 1.22 and 0.92, while $\mathcal{R}_{\mathcal{I}}^{\text{PCA}}$ had a median of 0.74, 0.64, 0.75 and 0.77 [IQR: 1.29, 0.65, 1.22 and 0.92] for T_a, T_{pe}, T_w and ST indices, respectively.

The $\mathcal{R}_{\mathcal{I}}^{\text{PCA}}$ values from the d_w and ST indexes, at the end of the occlusion, reached higher values. The median $\mathcal{R}_{\mathcal{I}}^{\text{PCA}}$ values, were 9.4, 7.7, 2.7, 3.0 and 12.0 for d_w, T_a, T_{pe}, T_w and ST indices, respectively.

To describe the prevalence of ischemia-induced changes during PCI, we analyzed the time instants at which the different indices began to show significant variations, that is, at what instant the different threshold values were exceeded. In this way, it was possible to analyze which indexes showed a more rapid response to ischemia-induced changes and at what time of occlusion it occurred. Table 3 shows the percentage of recordings where $\mathcal{R}_{\mathcal{I}}^{\text{PCA}}$ is larger than a given threshold $\alpha \in \{1, 5, 10\}$ at the end of balloon inflation, and the average time at which the threshold was exceeded.

Table 3: Classification of $\mathcal{R}_{\mathcal{I}}^{\text{PCA}}$ prevalence and time instant in which it was exceeded in the study population according to the different indices.

	% of patients with $\mathcal{R}_{\mathcal{I}}^{\text{PCA}}$			Average time (s) to reach $\mathcal{R}_{\mathcal{I}}^{\text{PCA}}$		
$\mathcal{I}$	> 1	> 5	> 10	> 1	> 5	> 10
d_w	94.1	64.4	48.5	17.4	34.7	51.8
T_a	88.1	61.4	41.6	18.7	38.6	46.3
T_{pe}	81.2	34.7	13.9	14.8	41.2	51.9
T_w	77.2	37.6	16.8	21.4	38.8	49.9
ST	89.1	67.3	54.5	14.6	33.7	44.2

The d_w values reached higher levels of sensitivity, measured by $\mathcal{R}_{\mathcal{I}}^{\text{PCA}}$, than the classic indices in a greater number of patients except for $\mathcal{R}_{\text{ST}}^{\text{PCA}}$ which reached 67.3% and the 54.5% for $\mathcal{R}_{\text{ST}}^{\text{PCA}} > 5, 10$, respectively. The least sensitive indices values into each thresholds were obtained for the indices T_a, T_{pe} and T_w, with T_{pe} being the lowest. For the indices with the highest prevalence (d_w and ST), detection in subset $\mathcal{R}_{\mathcal{I}}^{\text{PCA}} > 1$ occurred at 17.4 and 14.6 seconds, respectively after the onset of occlusion.

The temporal evolution of each index during ischemia was calculated as the evolution of the corresponding $\mathcal{R}_{\mathcal{I}}^{\text{PCA}}$ along balloon inflation every 5 seconds from the onset of occlusion. It was found that from the first moments of occlusion the $\mathcal{R}_{\text{T}_a}^{\text{PCA}}$, $\mathcal{R}_{\text{ST}}^{\text{PCA}}$ and $\mathcal{R}_{d}^{\text{PCA}}$ showed higher values corresponding to a stronger and faster response to the induced ischemia. The evolution of $\mathcal{R}_{\mathcal{I}}^{\text{PCA}}$ values averaged over the total study population are show in Fig. 8.

Figure 9 shows the percentage of patients presenting $\mathcal{R}_{\mathcal{I}}^{\text{PCA}} \geq 2, 5, 10$ for different occlusion times corresponding to times 1, 2, 3 and 4 min after balloon inflation. Note that the total number of recordings in each subset decreases over time due to the different occlusion times. The most important variations in the ECG seem to take place in the initial minute of occlusion in the indexes

studied, except for T_{pe} and T_w where only about 50% of patients exceed the threshold $\mathcal{R}_{\mathcal{I}}^{\text{PCA}} \geq 2$.

4 Discussion

This study evaluates the ability of the ventricular repolarization dispersion index, d_w, estimated from the peak to the end of the T-wave to characterize specifically the ischemia-induced dispersion of repolarization changes, thus avoiding the influence of ST segment elevation/depression. Using a warping-based assessment methodology we measure the T_{pe} morphological changes with respect to control, quantifying time course, lead distribution, and differences with classic biomarkers. Our main findings were that d_w, restricted to the T-wave peak-to-end, captures the changes between the peak and end of the T-wave, thus quantifying changes in ischemia-induced dispersion of repolarization, with impact on the regional differences in the spatial distribution of d_w according to the occluded artery. The d_w index better follow the ischemia-induced ECG variations than those classical indices that only consider information from specific ECG samples.

4.1 Time Course and Prevalence Analysis

The study of the time-course evolution of the d_w index confirmed its ability to robustly capture the variations of the T-peak to T-end morphology, hypothesized to specifically represent the ischemia-induced dispersion of repolarization changes, avoiding early T-waves and ischemia-induced ST elevation/depression changes.

A significant increase in the magnitude of d_w during PCI has been demonstrated as time elapses. As we actually expected, the ranges of values at control and during PCI were different: the d_w ranged in a narrow range in control, and in a wider range during PCI (see Fig. 5b). Moreover, the changes observed at the end of balloon inflation quantified using $\mathcal{R}_d^{\text{PCA}}$, estimated from d_w as described in (6), were (on median) 8 times larger than those obtained during the steady-state test at control recordings. The latter suggests that, in control conditions (without induced ischemic changes) the mean and standard deviation of $\mathcal{R}_d^{\text{PCA}}$ have small values since they only reflect normal ECG variability. The low values during the steady-state test at control recordings indicate a quite stable behavior (note that a value of 1 denotes a change in the second half comparable to the standard deviation in the first half).

In this work we have used different threshold values over $\mathcal{R}_d^{\text{PCA}}$ to quantify repolarization changes over-passing the threshold. It is important to note that threshold values for clinical use as risk markers require further experimental studies, in order to establish the level of normal variations such as changes induced by respiration, other underlying cardiac diseases, etc.

Different degrees of prevalence, where $\mathcal{R}_d^{\text{PCA}}$ was larger than certain thresholds were reported in Table 3, resulting in all cases statistically significant in

paired comparison between the PCI stage and the corresponding control stage, indicating that this index can be used to quantify ischemia-induced changes on ventricular repolarization from changes within their normal variations. Of the 86 patients who achieved $\mathcal{R}_d^{\text{PCA}} > 2$, 80.23% were within the first 30 seconds, supporting the hypothesis that variations in ventricular repolarization, quantified by d_w, could begin to appear very soon after the blood supply to a given part of the heart is compromised.

A greater range from the 75th to the 25th percentile of $\mathcal{R}_d^{\text{PCA}}$ was observed for the LAD occluded patients as compared to patients with other occluded arteries even of those changes were found no statistically significant possibly due to the small sample size. A larger study group as well as more information on the extent of the damaged area would be necessary to obtain relevant conclusions.

4.2 Spatial Analysis

The spatial distribution of d_w warping indicate how electrical activity is affected, as reflected in the T_{pe} interval, for the different occluded arteries. We found regional differences in the spatial distribution of d_w according to the occluded artery. The vast majority of the highest degrees of prevalence, both for $\mathcal{R}_d^l > 2$ and $\mathcal{R}_d^l > 5$, correspond to the region of the myocardium irrigated by the arteries as shown in Fig. 6, where higher prevalence of $\mathcal{R}_d^l$ index in leads $l \in \{\text{V1-V3}, \text{I}, \text{aVR}, \text{aVF}, \text{III}\}$ for RCA artery group and higher prevalence of $\mathcal{R}_d^l$ index in leads $l \in \{\text{V1-V3}, \text{V6}\}$ and marked decrease in aVR and III (inferior wall) for RCA artery group were found.

Regional differences were also found in the maximum d_w reached, depending on the occluded artery and the wall that the leads look at. Although the differences found were not strong, these findings suggest a certain capacity of the d_w index to indicate the location of the ischemia, considering also that different locations within the major artery were taken into account and there are no reports on the size of the damaged area. The lead distribution across the LAD and LCX subsets are in line with those reported in [13] using T-wave repolarization alternans analysis in the same study population.

The discrepancies in the spatial distribution of $\mathcal{R}_d^l$ and $\overline{d}_w^l$ (Fig. 6 and 7) can be attributed to patient-to-patient and lead-to-lead differences in σ_d^c, which quantifies the stability of the measurement during the control recording.

4.3 Classic Local Measurements

We have demonstrated that the warping-based d_w index, which takes into account all the morphological information of the entire interval studied, from T peak to T end, can better represent the ischemia-induced ECG variations than those indices that only consider information from specific ECG samples as T_{pe}. At the end of occlusion, $\mathcal{R}_{\mathcal{I}}^{\text{PCA}}$ values of 37.1, 13.9, 6.0, 5.6 and 27.7 were reached for d_w, T_a, T_{pe}, T_w and ST, respectively. $\mathcal{R}_d^{\text{PCA}}$ achieved higher values than those corresponding to classic indices (see also Fig. 8, Average of $\mathcal{R}_{\mathcal{I}}^{\text{PCA}}$ time-course). Only $\mathcal{R}_{\text{ST}}^{\text{PCA}}$ approached the value of $\mathcal{R}_d^{\text{PCA}}$, making the ST level the

measure based on fudicial points most sensitive to ischemic changes, as is already known in routine clinical practice where it is the most commonly used index. However, the underlying physiological mechanisms for ST elevation do not need to be the same as for T-peak to T-end interval morphology changes, as they reflect different physiological effects induced by ischemia. For ST segment elevation/depression, the mechanism can be the injury current generated by ischemia, while for the T_{pe} interval analysis the mechanism may be more related to repolarization dispersion generated by ischemia, also considered a surrogate for arrhythmia risk,

T_a, T_{pe} and T_w indices had the lowest values, and therefore, lower sensitivity. However, it must be taken into account that each index reflects different ischemia-related phenomena. Comparing $\mathcal{R}_d^{\mathrm{PCA}}$ with $\mathcal{R}_{\mathrm{T}_{pe}}^{\mathrm{PCA}}$, which are indices characterizing the same area of the T-wave, they reach values of the change index of 9.4 and 2.7, respectively, showing that d_w is more sensitive than T_{pe}, either because it betters reflect the underlying physiological changes, or because the stability of the measurement is higher or a combination of both reasons.

According to the data in Table 3, d_w and ST indices were also the most sensitive, with their corresponding $\mathcal{R}_{\mathcal{I}}^{\mathrm{PCA}}$ estimators exceeding the thresholds in a greater number of patients. The ST marker had the earliest reaction compared to any other index for all thresholds, however, the temporal differences of the indices achieving the threshold are not very wide ($<$ 8 s in all cases). Again the more meaningful comparison is between d_w and T_{pe}, having d_w the largest reaction, with no conclusive results in terms of early appearance.

The analysis of percentage of patients presenting $\mathcal{R}_{\mathcal{I}}^{\mathrm{PCA}} > 2, 5, 10$ for different occlusion times (see Fig. 9) discloses different degrees of prevalence of the studied indices when crossing different thresholds, with d_w and ST reaching the highest values, well in line with previous findings. From an overall perspective, it can be seen that, during the first minute, more than 60% of the changes appear, whereas in the second and third minute changes continue to increase but there is a deceleration in the rate of variations. As time progresses the number of patients with $\mathcal{R}_{\mathcal{I}}^{\mathrm{PCA}} > 2$ increases, d_w being the most sensitive in all cases, while there are others indices more sensitive than d_w for $\mathcal{R}_{\mathcal{I}}^{\mathrm{PCA}} > 5, 10$.

4.4 Clinical Implications

In this study we have available both control and induced ischemia ECG recordings. In clinical practice, however, it will be difficult to obtain non-ischemic control data to compare with, although d_w can still be computed with respect to a pre-ischemic ECG, if available, or with respect to a reference point like in this study where the reference is taken at the begging of the occlusion, allowing monitoring of T wave changes. In a scenario with available ECG recordings restricted to a stationary ischemia the methodology can not be applied. When applicable, the establishment of proper thresholds for d_w, under normal or ischaemic conditions, remains a challenge. Threshold values need to be established for detection or alarm triggering, and be applied to the raw d_w, or T_{pe}, not requiring a control recording. Note that the relative $\mathcal{R}_{\mathcal{I}}^{\mathrm{PCA}}$ magnitude is

used in this study just to characterize how d_w and T_{pe} changed during PCI as compared to changes in control, in order to determine their sensitivity.

Previous studies suggest that the T-peak-to-T-end interval is a strong ventricular arrhythmic marker in ischemic conditions [32]. This interval also avoids the location of T-onset in ischemia, which is very challenging due to the ST segment elevation/depression and early T wave modifications induced by ischemia. The index d_w aims to be an alternative to the T_{pe} interval in measuring ventricular repolarization dispersion more robustly. Further studies need to be designed to establish the proper thresholds to trigger arrhythmia alarms in clinical practice under ischemic conditions.

From Table 2 we see that men had larger $\mathcal{R}_d^{\text{PCA}}$ than women. We know that women have shorter T-peak-to-T-end interval values than men [33, 34], which possibly also implies a reduced dynamic range in T_{pe} prolongation induced by ischemia in women, congruent with the results shown in Table 2.

4.5 Limitations

The present study shows the power of d_w to monitor T-peak to T-end morphology changes induced by ischemia, and also that those changes are more prominently identified than by using other indices such as the T_{pe} interval. However, the study does not establish that d_w is as surrogate for arrhythmia risk marker under ischemia, since the occlusions were not long enough to generate arrhythmia. Other studies in animal models or other clinical scenarios should be tested to evaluate if the methodological sensitivity improvement of d_w with respect to T_{pe} translates to clinical superiority.

The proposed methodology is designed to capture morphological variations of the final part of the T wave that mainly represent an elongation. In this study we have not found any extreme ischaemia-induced T-peak-to-T-end variations affecting the method hypothesis. However, in addition to possible erroneous extraction of the T_{pe} interval morphology due to excessive noise and delineation errors, it can occur that subjects combining ischemia with other arrhythmia that causes modifications or alternations in the T wave final part (as moving from regular to biphasic, etc), can lead to misleading results as two different morphologies are fitted, not just prolonged T waves but including other deformations that prevent interpreting d_w as suggested in this work.

5 Conclusions

The T-wave time-warping based index, d_w, restricted to the T peak to end interval monitors ischemia-induced morphology changes of the final part of the T-wave, hypothesized to be a surrogate of repolarization dispersion changes. The observed increase in the d_w and $\mathcal{R}_d^{\text{PCA}}$ indexes during ischemia progression suggest its value as surrogate marker for the ischemia-induced increase of repolarization dispersion, requiring further clinical studies to evaluate its potential as ventricular arrhythmic risk marker during ischemia.

Acknowledgments

This work was funded by: a personal grant to N. Gomez from Santander Bank Latin American to Zaragoza University PhD program, and projects PID2019-104881RB-I00, PID2019-105674RB-I00 and TED2021-130459B-I00 by Spanish MICINN and FEDER, and BSICoS Group T39-20R, by Gobierno de Aragon, cofunded by FEDER 2014-2020 "Building Europe from Aragón". JR acknowledges funding from the European Union-NextGenerationEU and from Grant PID2021-128972OA-I00 funded by MCIN/AEI/10.13039/501100011033. Computations were performed by ICTS NANBIOSIS (HPC Unit 27 at University of Zaragoza).

References

[1] A. Alonso, F. H. J. Aparicio, E. J. Benjamin, M. S. Bittencourt, C. W. Callaway, F. A. P. Carson, F. A. M. Chamberlain, B. M. Kissela, F. K. L. Knutson, C. D. Lee, *et al.*, "Heart disease and stroke statistics—2021 update," *Circulation*, vol. 2021, no. 143, pp. e00–e00, 2021.

[2] A. Timmis, N. Townsend, C. P. Gale, A. Torbica, M. Lettino, S. E. Petersen, E. A. Mossialos, A. P. Maggioni, D. Kazakiewicz, H. T. May, *et al.*, "European society of cardiology: cardiovascular disease statistics 2019," *European heart journal*, vol. 41, no. 1, pp. 12–85, 2020.

[3] "Heart disease #1 cause of death rank likely to be impacted by covid-19 for years to come," tech. rep., American Heart Association, January 2021. `https://newsroom.heart.org/news/heart-disease`.

[4] O. Sayadi, D. Puppala, N. Ishaque, R. Doddamani, F. M. Merchant, C. Barrett, J. P. Singh, E. K. Heist, T. Mela, J. P. Martínez, *et al.*, "A novel method to capture the onset of dynamic electrocardiographic ischemic changes and its implications to arrhythmia susceptibility," *Journal of the American Heart Association*, vol. 3, no. 5, p. e001055, 2014.

[5] T. V. Kenttä, M. F. Sinner, B. D. Nearing, R. Freudling, K. Porthan, J. T. Tikkanen, M. Müller-Nurasyid, K. Schramm, M. Viitasalo, A. Jula, *et al.*, "Repolarization heterogeneity measured with t-wave area dispersion in standard 12-lead ECG predicts sudden cardiac death in general population," *Circulation: Arrhythmia and Electrophysiology*, vol. 11, no. 2, p. e005762, 2018.

[6] M. S. Fuller, G. Sandor, B. Punske, B. Taccardi, R. S. MacLeod, P. R. Ershler, L. S. Green, and R. L. Lux, "Estimates of repolarization dispersion from electrocardiographic measurements," *Circulation*, vol. 102, no. 6, pp. 685–691, 2000.

[7] J. M. Di Diego and C. Antzelevitch, "Acute myocardial ischemia: cellular mechanisms underlying ST segment elevation," *Journal of electrocardiology*, vol. 47, no. 4, pp. 486–490, 2014.

[8] J. Garcıa, P. Lander, L. Sörnmo, S. Olmos, G. Wagner, and P. Laguna, "Comparative study of local and Karhunen-Loève-based ST-T indexes in recordings from human subjects with induced myocardial ischemia," *Computers and Biomedical Research*, vol. 31, no. 4, pp. 271–292, 1998.

[9] S. Al-Zaiti, E. Sejdić, J. Nemec, C. Callaway, P. Soman, and R. Lux, "Spatial indices of repolarization correlate with non-ST elevation myocardial ischemia in patients with chest pain," *Medical & biological engineering & computing*, vol. 56, no. 1, pp. 1–12, 2018.

[10] O. Mazumder, D. Roy, and A. Sinha, "In silico cardiac model to evaluate myocardial ischemia effect on hemodynamic parameters," in *2020 28th European Signal Processing Conference (EUSIPCO)*, pp. 1105–1109, IEEE, 2021.

[11] M. N. Niemeijer, M. E. van den Berg, M. Eijgelsheim, G. van Herpen, B. H. Stricker, J. A. Kors, and P. R. Rijnbeek, "Short-term QT variability markers for the prediction of ventricular arrhythmias and sudden cardiac death: a systematic review," *Heart*, vol. 100, no. 23, pp. 1831–1836, 2014.

[12] M. Baumert, A. Porta, M. A. Vos, M. Malik, J.-P. Couderc, P. Laguna, G. Piccirillo, G. L. Smith, L. G. Tereshchenko, and P. G. Volders, "QT interval variability in body surface ECG: measurement, physiological basis, and clinical value: position statement and consensus guidance endorsed by the european heart rhythm association jointly with the esc working group on cardiac cellular electrophysiology," *Europace*, vol. 18, no. 6, pp. 925–944, 2016.

[13] J. P. Martínez, S. Olmos, G. Wagner, and P. Laguna, "Characterization of repolarization alternans during ischemia: time-course and spatial analysis," *IEEE Transactions on Biomedical Engineering*, vol. 53, no. 4, pp. 701–711, 2006.

[14] M. W. Rivolta, F. Rocchetta, L. T. Mainardi, F. Lombardi, and R. Sassi, "Quantification of spatial heterogeneity of ventricular repolarization during early-stage cardiac ischemia induced by coronary angioplasty," in *2019 41st Annual International Conference of the IEEE Engineering in Medicine and Biology Society (EMBC)*, pp. 4250–4253, IEEE, 2019.

[15] J. Ramírez, M. Orini, J. D. Tucker, E. Pueyo, and P. Laguna, "Variability of ventricular repolarization dispersion quantified by time-warping the morphology of the T-waves," *IEEE Transactions on Biomedical Engineering*, vol. 64, no. 7, pp. 1619–1630, 2016.

[16] J. Ramírez, A. Kiviniemi, S. van Duijvenboden, A. Tinker, P. D. Lambiase, M. J. Junttila, J. Perkiömäki, M. Orini, and P. B. Munroe, "ECG T-wave morphology variations predict ventricular arrhythmic risk in low- and moderate-risk populations," *JAHA: J Am Heart Assoc*, vol. 11, p. e025897, 2022.

[17] A. J. Moss, "Measurement of the QT interval and the risk associated with QTc interval prolongation: a review," *The American journal of cardiology*, vol. 72, no. 6, pp. B23–B25, 1993.

[18] W. Zareba, F. Badilini, and A. J. Moss, "Automatic detection of spatial and dynamic heterogeneity of repolarization," *Journal of electrocardiology*, vol. 27, pp. 66–72, 1994.

[19] J. E. Azarov, M. M. Demidova, S. Koul, J. van der Pals, D. Erlinge, and P. G. Platonov, "Progressive increase of the Tpeak-tend interval is associated with ischaemia-induced ventricular fibrillation in a porcine myocardial infarction model," *Europace*, vol. 20, p. 880–886, 2018.

[20] A. Mincholé, E. Pueyo, J. F. Rodríguez, E. Zacur, M. Doblaré, and P. Laguna, "Quantification of restitution dispersion from the dynamic changes of the T-wave peak to end, measured at the surface ECG," *IEEE Transactions on Biomedical Engineering*, vol. 58, no. 5, pp. 1172–1182, 2010.

[21] S. M. Narayan, "T-wave alternans and the susceptibility to ventricular arrhythmias," *Journal of the American College of Cardiology*, vol. 47, no. 2, pp. 269–281, 2006.

[22] E. Pueyo, P. Smetana, P. Caminal, A. B. de Luna, M. Malik, and P. Laguna, "Characterization of QT interval adaptation to RR interval changes and its use as a risk-stratifier of arrhythmic mortality in amiodarone-treated survivors of acute myocardial infarction," *IEEE Trans. on Biomedical Engineering*, vol. 51, no. 9, pp. 1511–1520, 2004.

[23] P. Brugada and J. Brugada, "Right bundle branch block, persistent ST segment elevation and sudden cardiac death: a distinct clinical and electrocardiographic syndrome: a multicenter report," *Journal of the American College of Cardiology*, vol. 20, no. 6, pp. 1391–1396, 1992.

[24] B. Acar, G. Yi, K. Hnatkova, and M. Malik, "Spatial, temporal and wavefront direction characteristics of 12-lead T-wave morphology," *Medical & biological engineering & computing*, vol. 37, no. 5, pp. 574–584, 1999.

[25] J. P. Martínez, O. Pahlm, M. Ringborn, S. Warren, P. Laguna, and L. Sörnmo, "The STAFF iii database: ECGs recorded during acutely induced myocardial ischemia," in *2017 Computing in Cardiology (CinC)*, pp. 1–4, IEEE, 2017.

[26] J. P. Martínez, R. Almeida, S. Olmos, A. P. Rocha, and P. Laguna, "A wavelet-based ECG delineator: evaluation on standard databases," *IEEE Transactions on biomedical engineering*, vol. 51, no. 4, pp. 570–581, 2004.

[27] P. Laguna, R. Jané, and P. Caminal, "Automatic detection of wave boundaries in multilead ECG signals: Validation with the CSE database," *Computers and biomedical research*, vol. 27, no. 1, pp. 45–60, 1994.

[28] S. Palacios, I. Cygankiewicz, A. Bayés-de Luna, J. P. Martínez, and E. Pueyo, "Sudden cardiac death prediction in chronic heart failure patients by periodic repolarization dynamics," in *2020 Computing in Cardiology*, pp. 1–4, IEEE, 2020.

[29] J. D. Tucker, W. Wu, and A. Srivastava, "Generative models for functional data using phase and amplitude separation," *Computational Statistics & Data Analysis*, vol. 61, pp. 50–66, 2013.

[30] A. Srivastava, W. Wu, S. Kurtek, E. Klassen, and J. S. Marron, "Registration of functional data using fisher-rao metric," 2011.

[31] D. P. Bertsekas, "Vol. 1 of dynamic programming and optimal control," *Athena scientific Belmont, MA*, 2005.

[32] J. E. Azarov, M. M. Demidova, S. Koul, J. Van Der Pals, D. Erlinge, and P. G. Platonov, "Progressive increase of the Tpeak-Tend interval is associated with ischaemia-induced ventricular fibrillation in a porcine myocardial infarction model," *EP Europace*, vol. 20, no. 5, pp. 880–886, 2018.

[33] M. Nakagawa, N. Takahashi, M. Watanabe, M. Ichinose, S. Nobe, H. Yonemochi, M. Ito, and T. Saikawa, "Gender differences in ventricular repolarization: terminal T wave interval was shorter in women than in men," *Pacing and clinical electrophysiology*, vol. 26, no. 1p1, pp. 59–64, 2003.

[34] M. Nakagawa, T. Ooie, B. Ou, M. Ichinose, H. Yonemochi, and T. Saikawa, "Gender differences in the dynamics of terminal T wave intervals," *Pacing and clinical electrophysiology*, vol. 27, no. 6p1, pp. 769–774, 2004.

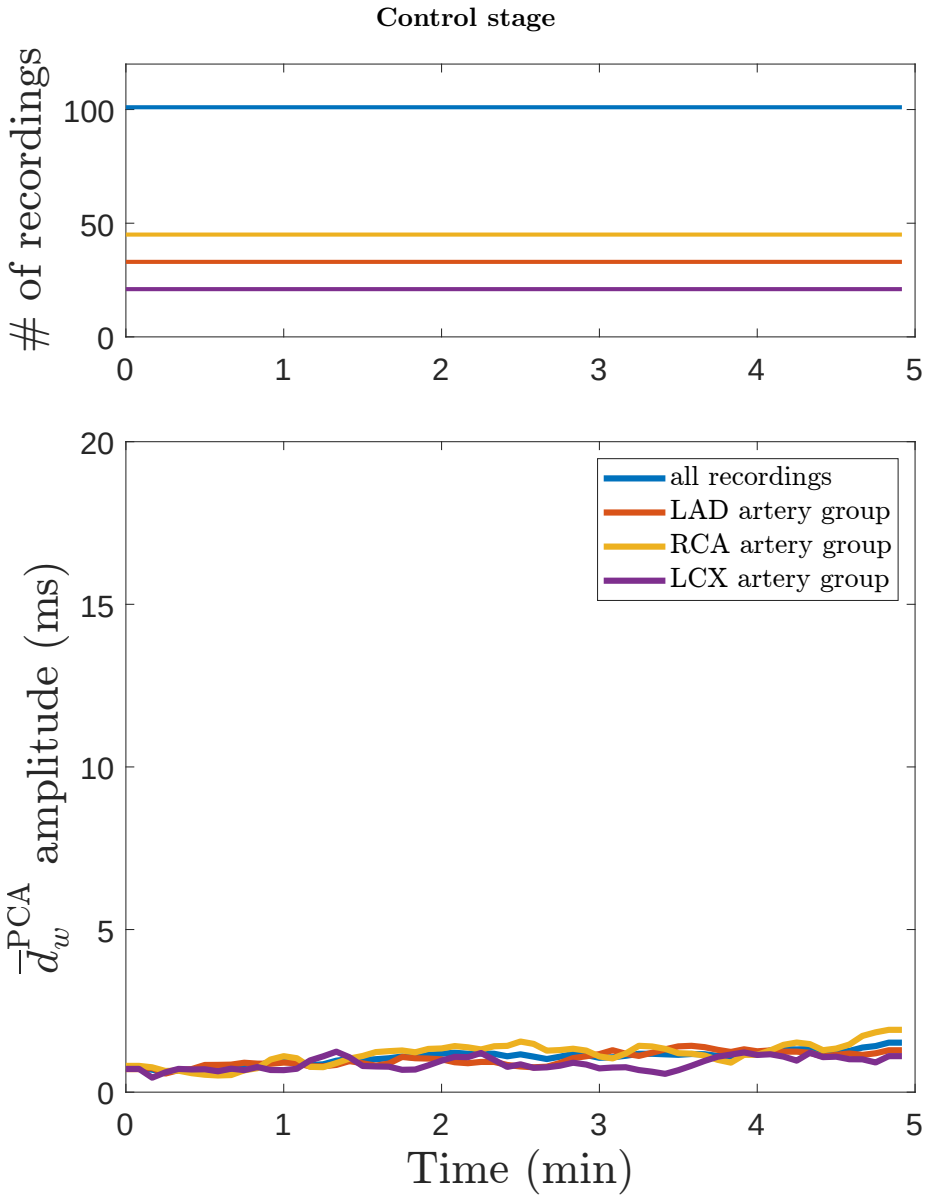
Control stage
# of recordings
100
50
0
0
1
2
3
4
5
20
15
10
5
0
all recordings
LAD artery group
RCA artery group
LCX artery group
$\overline{d}_w^{PCA}$ amplitude (ms)
Time (min)

(a)

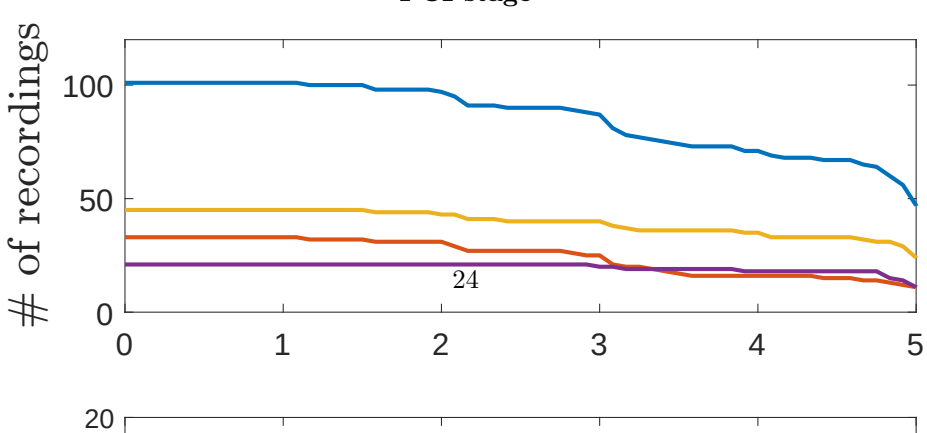
PCI stage
# of recordings
100
50
0
0
1
2
3
4
5
20
18
all recordings
LAD artery group
RCA artery group

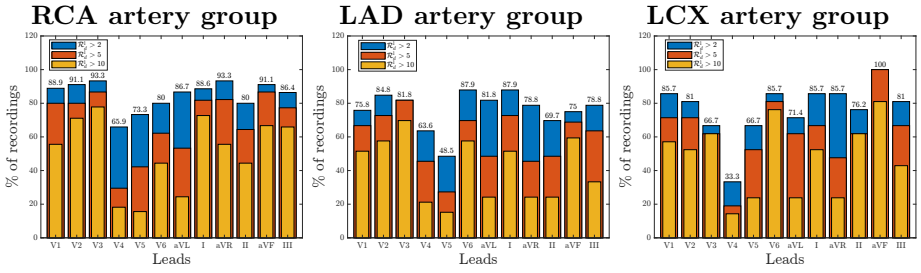

(a) (b) (c)

Figure 6: Percentage of patients with $\mathcal{R}_d^l > 2$ (blue bars), $\mathcal{R}_d^l > 5$ (red bars) and $\mathcal{R}_d^l > 10$ (orange bars) in each individual lead l measured at the end of occlusion and segregated by occluded coronary artery group: (a) RCA, (b) LAD and (c) LCX.

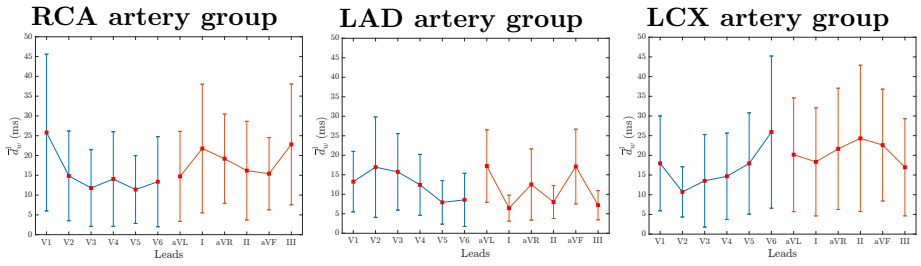

(a) (b) (c)

Figure 7: Average lead distributions of $\overline{d}_w^l$ in each occluded coronary artery, segregated by group: (a) RCA, (b) LAD and (c) LCX. The square represents the mean and the error bars represent ± standard deviation.

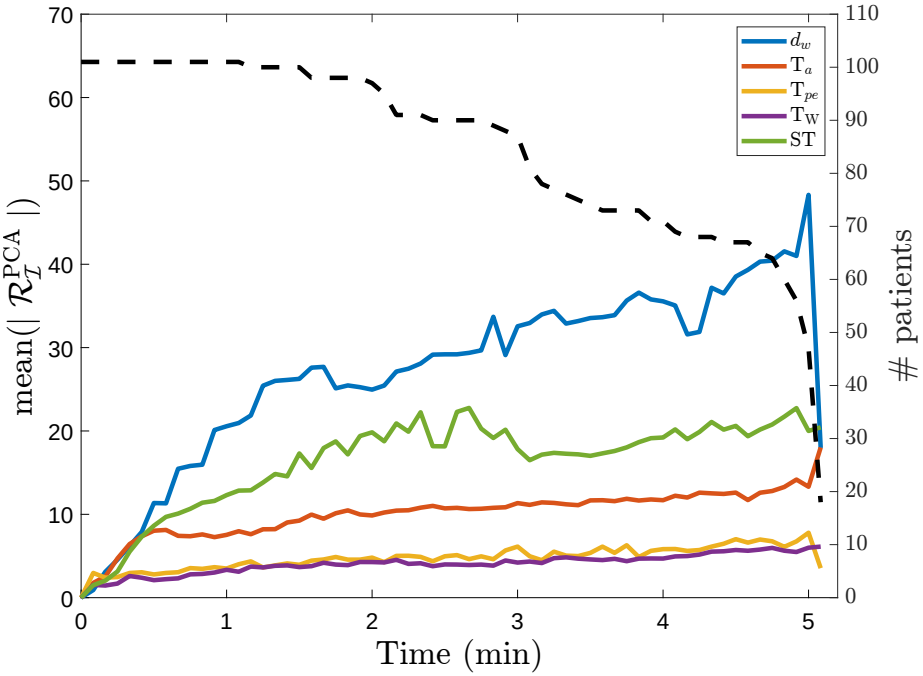

Figure 8: Average over patients of the $\mathcal{R}_{\mathcal{I}}^{\mathrm{PCA}}$ time-course aligned to the onset of the balloon inflation during PCI recording, and numbers of patients averaged at a given time. Dash black line and the left y-axis correspond to the number of averaged recordings.

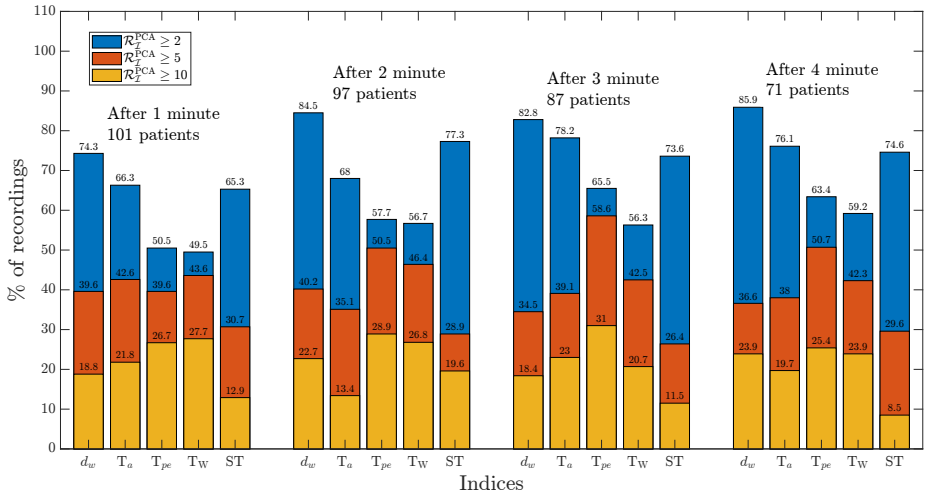

Figure 9: Percentage of patients with $\mathcal{R}_{\mathcal{I}}^{\mathrm{PCA}} \geq 2, 5, 10$ segregated by different occlusion times group: 1 min, 2 min, 3 min and 4 min after balloon inflation.